

From Pixels to Trajectory: Universal Adversarial Example Detection via Temporal Imprints

Yansong Gao, Huaibing Peng, Hua Ma, Zhiyang Dai,
Shuo Wang[†], Hongsheng Hu, Anmin Fu, Minhui Xue

Abstract—For the first time, we unveil discernible temporal (or historical) trajectory imprints resulting from adversarial example (AE) attacks. Standing in contrast to existing studies all focusing on *spatial (or static) imprints within the targeted underlying victim models*, we present a fresh temporal paradigm for understanding these attacks. Of paramount discovery is that these imprints are encapsulated within a single loss metric, spanning *universally* across diverse tasks such as classification and regression, and modalities including image, text, and audio. Recognizing the distinct nature of loss between adversarial and clean examples, we exploit this temporal imprint for AE detection by proposing **TRAIT** (Traceable Adversarial Temporal Trajectory Imprints). **TRAIT** operates under minimal assumptions without prior knowledge of attacks, thereby framing the detection challenge as a one-class classification problem. However, detecting AEs is still challenged by significant overlaps between the constructed synthetic losses of adversarial and clean examples due to the *absence of ground truth for incoming inputs*. **TRAIT** addresses this challenge by converting the synthetic loss into a spectrum signature, using the technique of Fast Fourier Transform to highlight the discrepancies, drawing inspiration from the temporal nature of the imprints, analogous to time-series signals. Across 12 AE attacks including SMACK (USENIX Sec’2023), **TRAIT** demonstrates consistent outstanding performance across comprehensively evaluated modalities (image, text, audio), tasks (classification and regression), datasets (nine datasets), and model architectures (e.g., ResNeXt50, BERT, RoBERTa, AudioNet). In all scenarios, **TRAIT** achieves an AE detection accuracy exceeding 97%, often around 99%, while maintaining a false rejection rate of 1%. **TRAIT** remains effective under the formulated *strong adaptive attacks*.

Index Terms—Adversarial Example Detection, Trajectory, Intermediate Models.



1 INTRODUCTION

Despite the exceptional performance of deep learning (DL) models, they confront threats from adversarial attacks [53], [58]. These attacks can result in unexpected behaviors such as adversarial example generation or backdoor implantation, or lead to privacy breaches in the underlying model or data such as through privacy inference attacks [12], [25], [43], [63]. The adversarial example (AE) attack has been a persistent security risk noted nearly a decade ago [74], coinciding with the rapid expansion of applications relying on deep learning. An adversary crafts an adversarial example by subtle perturbations to a benign example while

maintaining semantic similarity between them, for example, making the alterations imperceptible to humans when observing an adversarial image example. Initially demonstrated against image data types and classification tasks, AEs have extended their impact to various other data types such as audio [1], [35], text [24], [40], graphs [18], [85], and non-classification tasks [8], [71], [83], [90]. Consequently, this poses a significant threat to the security and safety of DL applications. These threats include breaching facial recognition [6], speech recognition [1] to gain unauthorized access, manipulation of self-driving systems [72], tampering with pedestrian detection [78], generating harmful text [51], evading malware and spam detection [14], and bypassing image safety checks in social networks to perpetuate cyberbullying [10].

Limitations of State-of-the-Art. Though significant strides have been made in developing countermeasures against such attacks, as outlined in the related work (section 11), current methods still face three notable limitations when it comes to neutralizing specific threats.

- *Limitation 1: Limited Prior Knowledge or Unseen Attacks.* A major limitation in current adversarial example defense approaches is their dependency on prior knowledge of AE techniques [46], [66], [95], especially evident in adversarial training and detection strategies. These methods often utilize insights from previously encountered AEs to enhance model robustness. While it improves resilience against known or similar attack patterns, its efficacy dimin-

- [†] Corresponding author.
- Y. Gao is with the School of Computer Science and Software Engineering, The University of Western Australia, Australia. garrison.gao@uwa.edu.au
- H. Peng, Z. Dai and A. Fu are with the School of Computer Science and Engineering, Nanjing University of Science and Technology, China. {paloze;dzy;fuam}@njjust.edu.cn
- H. Ma and M. Xue are with Data61, CSIRO, Australia. {mary.ma;jason.xue}@data61.csiro.au
- S. Wang is with the School of Cyber Science and Engineering, Shanghai Jiao Tong University, China. wangshuosj@sjtu.edu.cn
- H. Hu is with the School of Information and Physical Sciences, The University of Newcastle, Australia. hongsheng.hu@newcastle.edu.au

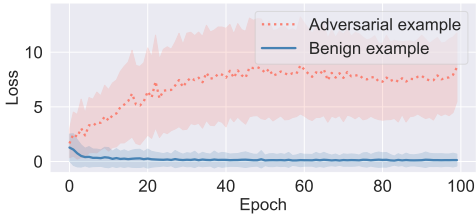


Figure 1: Losses of 1,000 clean and (untargeted) AEs on 100 intermediate models (CIFAR10+ResNet18). AE attack method is FGSM with $\epsilon = 8/255$ under ℓ_∞ -norm. Note the loss here is computed with the *ground-truth* label.

ishes significantly in the face of novel, unseen adversarial threats (especially adaptive attacks), highlighting a crucial limitation in defense without prior AE knowledge.

- **Limitation 2: Maintaining Primary Task Performance.** Enhancing DL model resilience through adversarial training often necessitates alterations in the training procedure or model architectures, diverging from conventional settings [50], [60], [65], [94]. Such modifications can introduce significant computational demands and potentially compromise the model’s performance on legitimate examples. Moreover, certain defense strategies that involve input preprocessing, like those requiring GANs [10], [86], [87] or diffusion models [89], face challenges related to training stability and high resource consumption, raising concerns about the practicality and efficiency of these approaches in preserving the primary task’s fidelity. This limitation in existing works demands a solution without undermining the primary task performance.

- **Limitation 3: Generalization cross Modalities or Tasks.** A significant portion of existing AE defense strategies, particularly those based on input transformations and detection mechanisms, are developed with a focus on image data, limiting their applicability across other modalities such as text and audio [33], [79], [80], [86], [87]. Additionally, there is a notable lack of defense methods capable of extending their protective measures beyond classification tasks to include other forms such as regression [46], [87], [94], highlighting the need for a more universally applicable solution.

Upon these prohibitive limitations, we throw the following research question:

Can we develop a universally applicable method for detecting AEs that operates efficiently and effectively across various modalities and tasks, independent of prior knowledge about specific attacks?

Technical Challenges. Upon examining existing literature (elaborated in section 11), we recognize that a solution to resolve the above research question is immensely challenging, perhaps even seemingly insurmountable. Traditional defense mechanisms primarily focus on spatial or static features within the model itself (i.e., they harness information from the *deployed underlying model solely* to detect AEs), neglecting the rich temporal information intrinsically available through the model’s training history. To address this challenging research question, it is important to resort to a *new paradigm* that leverages the temporal trajectories

imprinted by AEs during the model’s training phases. Model training involves multiple epochs, each producing an intermediate model (IM). While the final model is often used in deployment, these IMs, reflective of the model’s learning journey, are usually discarded. For the first time, we highlight that AEs leave distinct, traceable imprints within these temporal trajectories. When an AE is introduced to these IMs, its trajectory deviates from benign input. However, tapping these temporal imprints for AE detection still faces several technical challenges (Cs).

C1: Universal Metric for Trajectory Imprints. Identifying a metric that consistently reflects trajectory imprints universally across different tasks and modalities is challenging. Conventionally used metrics like latent representations, logits, and softmax values, while informative, are high-dimensional and may become unwieldy, especially in scenarios with a vast number of categories like facial recognition. Furthermore, their applicability can be limited by model architecture and task specificity, rendering some metrics, such as softmax values, unsuitable in contexts like regression tasks.

C2: Distinguishability of Overlapping Loss Imprints. The task of differentiating benign inputs from AEs becomes particularly challenging due to the substantial overlap observed in their loss trajectories over the model’s training epochs. This overlap, as illustrated in Figure 2 and Figure 3, makes it difficult to identify adversarial interventions. The root of this challenge is the *absence* of explicit ground-truth for online incoming data, which would otherwise provide a clear benchmark for comparison. Without this definitive reference, the loss imprints of adversarial and benign examples appear deceptively similar, complicating the detection process.

C3: Navigating Uncharted Attacks. A recognized challenge in adversarial defense is the absence of prior knowledge about new or evolving adversarial techniques. This lack of insight into the continually advancing landscape of adversarial strategies poses a significant barrier to creating defenses that are resilient to evolving threats. Traditional defense mechanisms often rely on known attack patterns to train and fortify models, leaving them vulnerable to unseen attacks, especially adaptive attacks.

Our Solution. Through a meticulous examination of the outlined challenges, we have developed a framework that proficiently identifies AEs, seamlessly extending its capabilities across diverse data modalities, tasks, and model architectures with preserved efficiency and effectiveness.

To address the first challenge **C1**, we resort to the loss as a universal metric to quantify the trajectory imprint. The loss metric stands independent of model architecture, task and modality, offering a standardized universal measure to characterize the trajectory imprint, circumventing the complexities associated with high-dimensionality and task-specific dependencies. As exemplified in Figure 1, it displays the losses of 1,000 adversarial and clean examples across about 100 IMs where the *ground-truth is assumed to be known*. We can see that the loss curves are different between them. The significant disparity in the loss imprint between adversarial and benign examples appears promising. However, a critical factor to note is the absence of ground-truth for incoming inputs, making direct loss computation impossible.

We overcome it via *synthetic loss*, where the predictions from the target model serve as the surrogate ground-truth (as elaborated in subsection 2.2). However, synthetic loss poses the challenge **C2**, where the loss imprints of adversarial and clean examples become substantially overlapped.

To mitigate the second challenge **C2**, our approach involves initially employing noise suppression to enhance the signal-to-noise ratio. Subsequently, transforming the temporal imprints, inspired by their similarity to time-series signals, into the spectrum domain is undertaken to amplify the discernible differences (as detailed in subsection 2.2).

To address the third challenge **C3** to ensure the efficacy against all forms of AE attacks, it is crucial *not* to assume any prior knowledge of these attacks. We resolve this by framing adversarial sample detection as an anomaly detection problem. Leveraging a deep support vector data description (deep SVDD) trained solely on imprints derived from benign examples as a single-class classifier (as elaborated in subsection 3.2), we tackle this challenge head-on.

Contribution: Our main contributions are threefold¹:

- To the best of our knowledge, TRAIT pioneers the exploration of traceable temporal imprints to characterize adversarial behaviors, a significant change from existing methods that focus solely on spatial imprints. This novel paradigm not only overcomes several limitations of existing methods but also keeps the integrity of the protected model and its training procedure intact.
- By integrating temporal imprints into a universally adaptable loss metric and enhancing the differentiation between adversarial and benign examples through innovative techniques, we introduce the TRAIT framework that operates effectively without prior AE knowledge. By design, TRAIT is independent of data modalities, tasks, and model architectures, marking a significant advancement in adversarial defense.
- Comprehensive evaluations validate the exceptional performance of TRAIT in detecting AEs with high accuracy and efficiency across different modalities, including images, audio, and text on up to 12 diverse attacks (including new audio AE attack of SMACK [88]). TRAIT consistently achieves exceptional performance regardless of diverse datasets (four imagery including CIFAR10, STL10, CIFAR100 and TinyImageNet, two audio, and one textual classification datasets, and two regression datasets) and model architectures (e.g., ResNeXt50, BERT, RoBERT). For all cases, TRAIT exhibits an AE detection accuracy exceeding 97%, often around 99%, maintaining a low false rejection rate of 1%, underscoring its robustness and reliability. In addition, TRAIT demonstrates high resilience against strong adaptive attacks.

2 INSIGHTS

This section begins with an overview of our key **insights and motivation**, highlighting the significance of universal temporal trajectory imprints subsection 2.1 imprinted by AEs and their encapsulation within a universal loss metric subsection 2.2. Inspired by these insights, we address two critical challenges of **C1** and **C2**, with the motivation of harnessing this universal metric to effectively identify AEs.

1. Source code will be released upon publication of this work.

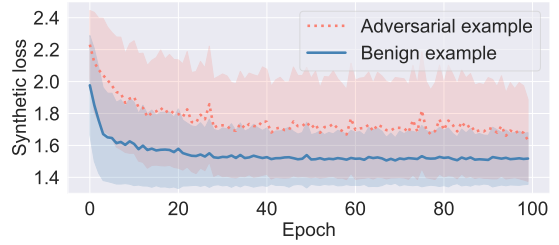


Figure 2: Synthetic losses of 1,000 clean and (untargeted) adversarial examples, respectively, on 100 intermediate models. Other settings are the same to Figure 1.

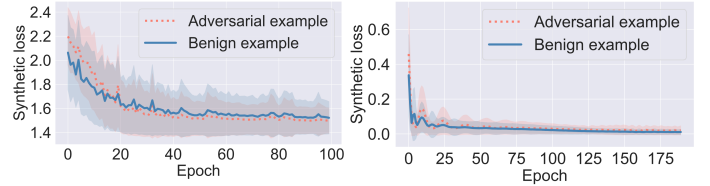


Figure 3: Synthetic loss of (left) classification task of STL10 with ResNet18, and (right) multivariate time-series regression task, temperature forecasting with LSTM.

2.1 New Signal: A Universal Temporal-Trajectory Imprint

AEs, regardless of their generation methods, are designed to exhibit noticeable deviations from the normal data distribution, thus impacting inference results. Our exploration introduces a fresh perspective on identifying these deviations through trajectory imprints left across intermediate models (IMs) intrinsically rooted in the training procedure.

We specifically examine temporal-trajectory imprints captured by IMs at each training epoch. These imprints, serving as historical markers, reflect the model’s evolution and only require preservation for analysis. Despite their similarities to the final deployed model, IMs offer unique insights with their epoch-specific parameter variations.

While various imprints like latent representations, logits, and softmax values are informative, they present challenges such as high dimensionality in scenarios with extensive class categories, or applicability limitations to common tasks like regression. In contrast, the loss metric stands out for its universal applicability and consistent lowest dimensionality across different tasks, making it an ideal candidate for a universal metric. This approach leverages the foundational role of loss functions in guiding the training process, addressing the challenge **C1** by adopting a loss-based imprint that transcends task and modality boundaries.

2.2 Synthetic Loss: A Universal Temporal Imprint Metric

A significant hurdle in this pipeline is the *absence of ground truth* for incoming examples during inference, whether benign or adversarial, rendering the computation of their actual loss unfeasible. We note that works used trajectory for membership inference attacks [43] or countering poisoning attacks [41] all require the available ground-truth as a must to fulfill their objectives. However, such a ground-truth is

unavailable in our case. To circumvent this, we propose *synthetic loss*, which diverges from the traditional loss computation that relies on known ground-truth annotations, such as labels. For tasks like classification or regression, this involves leveraging the output probabilities or predicted values from the target model as a ‘surrogate ground-truth’, for each IM to compute the synthetic loss. Moreover, we have delved into additional strategies for synthesizing loss, which are elaborated upon in the subsection 10.3.

An example of synthetic loss imprinted trajectory across IMs in a classification scenario is demonstrated in Figure 2. This synthetic loss context mirrors the setup in Figure 1 that assumes the known ground-truth. Compared with Figure 1, two critical observations emerge:

Observation 1: *The synthetic losses for adversarial and benign examples exhibit differences not only in their magnitude but also in the patterns of their fluctuations .*

Observation 2: *The clarity in distinguishing between adversarial and benign examples diminishes when employing synthetic loss, in contrast to the distinct separations with actual loss computations in Figure 1 .*

■ **Addressing C1.** The *Observation 1* underscores the potential of leveraging *synthetic loss* as a universal metric for real-time identification of AE, without the need for additional training or alterations to the target model. Crucially, this approach bypasses the requirement for ground truth in loss computation, effectively overcoming challenge **C1**.

■ **Addressing C2.** The *Observation 2*, however, poses a new challenge **C2**: trajectory imprints between benign and adversarial examples can be (significantly) overlapped, resulting in low distinguishability. We note that this imprint overlapping can be severe for some AE attacks or dependent on tasks e.g., regression. We have shown the synthetic loss imprint of a regression task (multivariate time-series forecasting) across IMs in Figure 3 (right)—experimental settings are detailed in subsection 4.1. We have also additionally shown the synthetic loss imprint of STL10 in Figure 3 (left), where the overlapping is extremely severe.

Nonetheless, the imprints left by AEs do differ from those of benign instances. IMs corresponding to early epochs still demonstrate relatively high randomness—different trends for adversarial and benign examples—without exhibiting substantial convergence. *In essence, AEs, not originating from the same distribution as clean examples, manifest discernible statistical temporal-trajectory imprints.* Consequently, the challenge **C2** persists but may be effectively addressed by amplifying the temporal synthetic loss distinguishability. Two primary techniques are proposed to tackle challenge **C2**:

- **Noise Suppression:** The raw synthetic loss imprint contains noise, requiring salient feature extraction to enhance the signal-to-noise ratio. Therefore, we employ an LSTM auto-encoder for noise reduction, focusing on extracting critical features to improve the signal-to-noise ratio (SNR).
- **Spectrum Transformation:** In signal processing, transforming a time-series signal from the time-domain to the frequency/spectrum domain often reveals more distinct features. Given that loss imprints inherently resemble time-series data, applying spectrum transformation aligns naturally

with their temporal characteristics, offering a promising avenue for addressing the challenges in AE detection. Accordingly, we constructively transform the dimensionality-reduced synthetic loss feature into a spectrum to further accentuate the distinguishability between adversarial and benign examples. Equally, it further enhances the SNR.

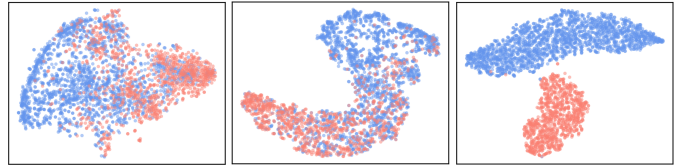


Figure 4: T-SNE visualization of benign and adversarial examples of (left) synthetic loss, (middle) after noise suppression, and (right) after spectrum transformation. Benign examples are with cornflowerblue color and adversarial examples are with salmon color. *Quantitative evaluations* of the role of noise reduction and spectrum transformation are detailed in subsection 9.1.

Visualization and Qualitative Analysis. We illustrate the effect of noise suppression and spectrum transformation on the setting presented in Figure 2. Leveraging t-SNE [76], we project both adversarial and benign examples onto a two-dimensional space, as depicted in Figure 4. Notably, the synthetic losses showcased in Figure 4 (left) demonstrate a considerable overlap between adversarial and benign examples. In addition, the two clusters are not apparent.

Following noise suppression, executed through an LSTM-encoder outlined in subsection 3.3 for salient feature embedding, the overlap diminishes noticeably. Consequently, the two clusters become denser, as visualized in Figure 4 (middle). Subsequently, upon transformation into the spectrum domain utilizing Fast Fourier Transform, a clear separation emerges between adversarial and benign examples, as demonstrated in Figure 4 (right). It’s important to note that in this spectrum depiction, only the amplitude information is displayed, while the phase information remains omitted.

3 TRAIT

Having navigated through challenges **C1** and **C2**, we uncover a viable path for utilizing synthetic loss as a means to identify AEs post-deployment of the target model. This motivates us to develop TRAIT framework. We begin by defining the threat model and addressing the last remaining challenge, **C3**. Subsequently, we overview and detail the TRAIT.

3.1 Threat Model

Attacker: We consider a strong attacker, who is endowed with in-depth, white-box knowledge of the target model. This knowledge allows for the execution of advanced white-box AE attacks. Despite this profound insight, the attacker is barred from accessing the IMs (relaxed in adaptive attacks in Section 7), which, though not as potent as the final model, contain valuable temporal data reflective of the model’s training trajectory. The attacker is unconstrained by computational limits or the extent of perturbation applied to craft

AEs, with a general preference for subtler modifications to ensure the deceptive alterations remain undetectable, thereby preserving the semantic integrity of the adversarial inputs.

Defender: The defender is typically the entity deploying the model. Their arsenal is limited to the deployed model, referred to as the target model, and its intermediate states, without the liberty to alter its training dynamics or access insights into the methodologies used by attackers for crafting AEs. This setup places the defender in a challenging position, armed with minimal knowledge, primarily relying on the IMs naturally generated at each training epoch and then preserved. These IMs, while not as refined as the final model, serve as a crucial resource for the defender and are preserved for potential defensive utility.

3.2 Overview of TRAIT

■ **Addressing C3.** The absence of prior knowledge of AE crafting methods constitutes the third challenge, **C3**. This situation leaves the defender reliant solely on the analysis of benign examples’ temporal trajectory imprints. To overcome **C3**, we integrate anomaly detection, specifically employing the SVDD [62], [75] model. The SVDD is meticulously trained on the refined and spectrally transformed imprints of benign examples, ensuring a focused and effective detection mechanism. By addressing **C3** in conjunction with the previously circumvented challenges **C1** and **C2**, we lay a solid foundation for the development of TRAIT, effectively equipping it to identify and mitigate adversarial threats without any prior knowledge of AE generation techniques.

The overview of TRAIT is depicted in Figure 5, consisting of two phases: the offline phase and the online phase. The former phase establishes an anomaly detector that identifies the AEs as anomalies throughout the subsequent online phase.

3.2.1 Offline Phase

During the offline phase, the model provider trains the DL model M with K epochs, the same as the typical training procedure. Each intermediate model, IM, per epoch is preserved by the provider. At the end of the training, there are K IMs, $\{IM_1, \dots, IM_k, \dots, IM_K\}$. The IM_k often serves as the final model M to be deployed in practice. Note that, the deployed model M can be the intermediate model generated at any epoch (usually close to the k_{th} epoch), for example, with the highest validation accuracy.

In step ①, the model provider randomly selects a subset of n validation examples (e.g., images), where $n = e.g., 1000$, that are correctly classified as benign by the target model to their ground-truths. These examples are utilized as benign instances, excluding misclassified ones to mitigate noise. Each benign example undergoes evaluation by all K IMs. Subsequently, the synthetic loss for each k_{th} IM is calculated based on the softmax vectors in a classification task or the predicted value in a regression task, involving both the k_{th} IM and the target model M . Typically, the target model M corresponds to the K_{th} IM. Consequently, for each benign example, $K - 1$ synthetic loss elements are generated.

In step ②, the synthetic loss imprints of the n benign examples are leveraged to train an encoder-decoder

pair. Here, the bottleneck of this pair denotes the low-dimensional feature, termed the embedding, designed for noise reduction purposes. Subsequently, these embeddings undergo transformation into the spectrum domain and are utilized to train the SVDD. The SVDD functions as a single-class classifier, to detect AEs devoid of any prior knowledge regarding their attack methods. It’s noteworthy that the pre-set false rejection rate—defined as the rate of falsely rejecting a benign example as an adversarial example—serves as a hyperparameter of the SVDD during its training phase.

3.2.2 Online Phase

This phase is relatively straightforward. Given an incoming example, whether adversarial or benign, it is fed into all IMs to acquire the synthetic loss imprint trajectory (e.g., $K - 1$ elements). This loss trajectory is embedded by the encoder, and the resulting embedding is transformed into the spectrum domain before being fed into the SVDD that judges whether the input is benign or adversarial.

3.3 Key Component Implementation

The second step ② during the offline phase holds significant importance, encompassing two pivotal components: the discriminability intensifier and the deep-SVDD. The discriminability intensifier is comprised of an autoencoder and the spectrum transformation, which aims to enhance the discriminability between AE synthetic loss trajectory-imprints and benign counterparts. On the other hand, the deep-SVDD serves as an anomaly detector to identify AEs.

Discriminability Intensifier consists of two parts: an encoder for low-dimensional synthetic loss embedding operation and a spectrum transformation operator. For the former, The use of an encoder to reduce dimensionality and extract salient features is primarily aimed at capturing essential information while discarding noise or irrelevant details in the synthetic loss imprint. Training an encoder-decoder pair facilitates this process by compressing the synthetic loss imprint into a lower-dimensional space (embedding) using the encoder, focusing on the most salient feature of the input. As the synthetic loss imprint is akin to a time-series signal, we thus leverage an LSTM-based encoder to perform the embedding. More specifically, we use a 2-layer bi-directionally structured LSTM model as the autoencoder for synthetic loss imprint noise and dimension reduction. In order to prevent the model from overfitting, a dropout value of 0.2 was applied to both the encoder and decoder. The number of training epochs is 150. Note the autoencoder training is fast. Also note that the decoder is no longer needed in the online phase of TRAIT, shown in Figure 5. Because now only the encoder is required for the embedding operation. The latter spectrum transformation is through the FFT. Inspired by the fact that time-series signal analysis can be more efficient in the spectrum domain and the temporal imprints can indeed be treated as time-series signals along the epoch-axis.

Deep-SVDD [62] is a variant of the classical SVDD algorithm that extends its application to high-dimensional data by utilizing deep neural networks. Deep SVDD aims to learn a representation of normal (non-anomalous) data instances in a lower-dimensional space, often called the embedding

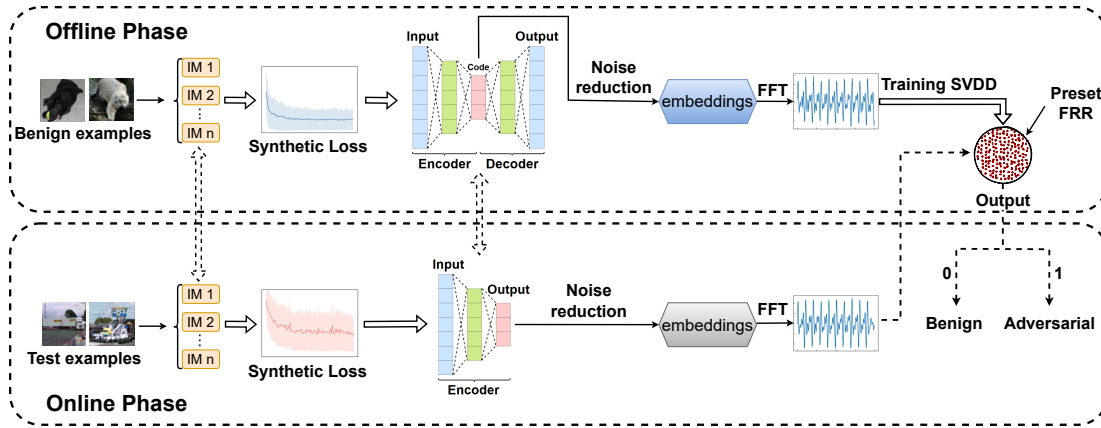


Figure 5: The TRAIT overview. The IM stands for an intermediate model of the underlying/victim model.

space or hypersphere, while simultaneously minimizing the volume of this space. By doing so, it captures the most essential characteristics of the normal data, allowing anomalies to be detected as instances that fall outside this learned normality region in the embedding space.

The Deep-SVDD incorporates a preset FRR as one of its input hyperparameters². The defender has the flexibility to set a small FRR (for example, 1-3% in practical scenarios) during the Deep-SVDD training. This FRR signifies the acceptable probability that a benign example might be incorrectly classified as an AE, resulting in rejection. It’s important to note that the trained Deep-SVDD operates as a binary classifier, making decisions based on its learned threshold to distinguish between adversarial and benign examples.

4 EVALUATION

This section extensively evaluates TRAIT with image classification tasks. Its cross-modality and cross-task capability are affirmed in Section 5 and Section 6, respectively.

4.1 Setup

Dataset. While two widely used benchmark datasets of CIFAR10 [36] and STL10 [16] are extensively evaluated herein, we have evaluated CIFAR100 (see subsection 9.3) and TinyImageNet (see subsection 10.1). STL10 has 13,000 color images of size $96 \times 96 \times 3$. The training and test sets have 5,000 and 8,000 images, respectively, with 10 classes in total. The CIFAR10 dataset consists of 60,000 color images of size $32 \times 32 \times 3$ in 10 classes, with 6,000 images per class. There are 50,000 training images and 10,000 test images.

Attack. We evaluate TRAIT up to 7 mainstream AE attacks: 6 white-box and 1 black-box. Specifically, the white-box adversarial examples include Fast Gradient Sign Method (FGSM) [26], Projected Gradient Descent (PGD) [49], Basic Iterative Method (BIM) [37], Carlini and Wagner Attack (CW) [13], DeepFool [54], Jacobian Saliency Map Attack

(JSMA) [57]. The black-box adversarial example attack is Boundary attack [11]. Each attack is detailed in Appendix A.

All these AE attacks use l -norm (e.g., l_0 , l_1 , l_2 and l_∞) as perturbation constraints or measurements [48]. In our evaluations, the l_2 -norm is set for DeepFool, l_0 -norm is set for JSMA, and l_∞ -norm is set for FGSM, BIM, PGD, CW, and Boundary attacks. Note that the perturbation magnitude ϵ can be flexibly configured for FGSM, BIM, and PGD. While for other AE attacks, the ϵ is usually fixed.

Model. We use ResNet18 [32] for extensive evaluations in this section, while we have also taken VGG16 [69] for generalization evaluations.

Machine. The experiments were implemented on the DL framework PyTorch 1.13.1 and Python 3.9. The machine is a LENOVO laptop with an AMD Ryzen 7 5800H CPU (8 logical cores) and 16GB DRAM memory, and a GeForce GTX 1650 GPU (4GB video memory).

Metric. The metrics of detection accuracy and false rejection rate (FRR) are pivotal for assessing the effectiveness of TRAIT’s performance. Detection accuracy quantifies the likelihood of correctly identifying adversarial examples (AEs) as such. Conversely, the FRR gauges the likelihood of erroneously categorizing benign examples as AEs, leading to their rejection. Ideally, detection accuracy should approach 100%, while the FRR should be minimized to 0%.

4.2 Results

We first show and interpret the results of CIFAR10 using ResNet18 model and then the results of STL10 and a different VGG16 model. All results are summarized in Table 1.

CIFAR10. We conducted ResNet18 training for 104 epochs. The final model from the last epoch is utilized as the target model, exhibiting a classification accuracy of 94.03%.

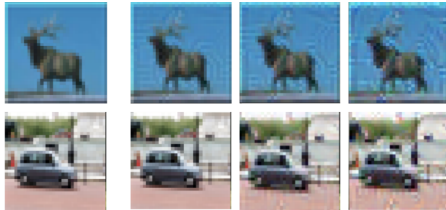
We use the Adversarial Robustness Toolbox³ to implement these AE attacks. For all six white-box AE attacks, we use 3000 benign examples to generate adversarial examples per AE attack; the number of AEs depends on the attack success rate for each type of AE attack, e.g., varying from 77% to 96%. For configurable ϵ , we have set it to 8/255 and 16/255, respectively. These are preferable in practice by the attacker as the perturbation injected remains

2. The Deep-SVDD is adopted from https://github.com/yzhao062/pyod/blob/master/examples/deepsvdd_example.py. The SVDD function parameter `contamination` represents the preset percentage of benign samples being tolerated to be outliers, which is the preset FRR.

3. <https://github.com/Trusted-AI/adversarial-robustness-toolbox>

Table 1: TRAIT detection performance (CIFAR10+STL10).

AE attack Method	Perturb Magnitude	Preset FRR(%)	AE Acc(%)		
			CIFAR10		STL10
			ResNet18	VGG16	ResNet18
BIM (ℓ_∞ -norm)	$\epsilon = 8/255$	1	97.94	98.61	97.88
		3	98.66	98.89	98.12
		5	99.11	99.37	98.62
	$\epsilon = 16/255$	1	97.95	98.43	97.21
		3	98.32	98.81	97.86
		5	98.84	98.95	98.44
FGSM (ℓ_∞ -norm)	$\epsilon = 8/255$	1	98.31	99.01	98.16
		3	98.80	99.33	98.33
		5	99.38	99.41	99.11
	$\epsilon = 16/255$	1	99.75	99.35	99.23
		3	99.76	99.72	99.41
		5	99.89	99.84	99.44
PGD (ℓ_∞ -norm)	$\epsilon = 8/255$	1	97.45	98.79	97.46
		3	98.01	99.11	98.82
		5	98.33	99.24	98.91
	$\epsilon = 16/255$	1	96.44	98.28	96.26
		3	96.89	98.56	96.45
		5	97.22	98.76	97.03
CW (ℓ_∞ -norm)	-	1	99.76	99.64	99.42
		3	99.76	99.81	99.59
		5	99.83	99.86	99.71
DeepFool (ℓ_2 -norm)	-	1	99.59	99.31	99.46
		3	99.70	99.44	99.53
		5	99.71	99.72	99.64
JSMA (ℓ_0 -norm)	-	1	99.56	99.64	99.62
		3	99.67	99.68	99.78
		5	99.78	99.77	99.96
Boundary (ℓ_∞ -norm)	-	1	99.73	99.15	98.09
		3	99.89	99.62	98.43
		5	99.97	99.78	98.77



Benign example Adversarial example

Figure 6: (Left) benign examples and (Right) their adversarial examples. From left to right, $\epsilon = 8/255, 16/255$ and $32/255$, respectively. AE method is BIM.

imperceptible—the perturbation appears to be perceptible when $\epsilon = 32/255$, as demonstrated in Figure 6, $\epsilon = 32/255$ changed the image significantly compared to $\epsilon = 16/255$ and $8/255$.

Considering the large amount of time/computation required to implement the black-box AE attack (in particular, the Boundary attack), we only select 200 samples in the test dataset (which takes about 10 hours) to generate AEs.

We have preset the FRR at 1%, 3%, and 5%, respectively. As expected, there exists a trade-off where the detection accuracy tends to increase with higher FRR values. Remarkably, for CW, DeepFool, JSMA, and Boundary attacks, the detection accuracy is consistently near 100%, even at an FRR as low as 1%. It’s important to note that the FRR is pre-set offline, aligning consistently with the online FRR measured using benign examples. Regarding FGSM, the detection accuracy remains above 98% across various perturbation magnitude configurations, even at an FRR of 1%. For BIM

and PGD attacks, the observed drop in detection accuracy is negligible (within 1%) compared to FGSM. Despite the stealthier nature of BIM and PGD attacks owing to their interactive perturbation injection, TRAIT demonstrates efficient capture capabilities against these methods.

STL10. We conducted training on ResNet18 using STL10 for 120 epochs, resulting in the last epoch model or target model achieving a classification accuracy of 76.89%. To generate AEs for each white-box AE attack, we randomly selected 2000 benign samples. However, due to the significant computational and time overhead, we used only 200 benign examples (approximately 30 hours) to generate the AEs for the Boundary attack, the black-box attack. For the adjustable parameter ϵ , we set it to $8/255$ and $16/255$, respectively.

Even when considering a 1% preset FRR, the detection accuracy remains consistently above 97% against all AE attacks, as shown in the settings outlined in Table 1. Notably, the detection performance on STL10 closely resembles that observed on the CIFAR10 dataset. This suggests that TRAIT exhibits invariance across datasets.

VGG16. We conducted training on VGG16 using CIFAR10 for 105 epochs. The final model from the last epoch, which achieved a classification accuracy of 93.95%, is deployed as the target model. The settings identical to those used to generate AEs for the ResNet18 model were employed to create AEs for the VGG16. As depicted in Table 1, the performance of TRAIT on VGG16 closely resembles that of ResNet18. This suggests that TRAIT exhibits invariance not only across different dataset configurations but also across varying model architectures.

5 CROSS-MODALITY TASKS

This section validates the inherent generic capability of TRAIT across different modalities including audio and text.

5.1 Audio

Setup. For the audio modality, the dataset of AudioMNIST [9] is used. It consists of 30,000 audio samples of speech digits (0-9) from 60 different speakers. We implemented the task of recognizing 0-9 speech digits with AudioNet [9]. Training and test datasets each have 25,000 and 5,000 samples.

Results. We conducted training on AudioNet utilizing the AudioMNIST dataset for a total of 50 epochs. The final model obtained from the last epoch, which achieved a classification accuracy of 95.40%, serves as the target model.

To generate AEs, we randomly selected 2000 benign audio samples. The implementation of adversarial attacks involved perturbing speech samples using six white-box AE methods: FGSM, PGD, BIM, CW, DeepFool, and JSMA. The AE attack generation toolbox is the same as for the image dataset. It’s important to note that all these attacks are untargeted. Exemplified adversarial audio waveforms are depicted in Fig. 13 in the Appendix, which are almost similar to their benign ones.

For each of the six AE attacks, we assessed the efficacy of TRAIT in detecting audio AEs by setting the FRR to predetermined levels of 0.5%, 1%, 3%, and 5%, respectively. The performance results are illustrated in Figure 7. It is

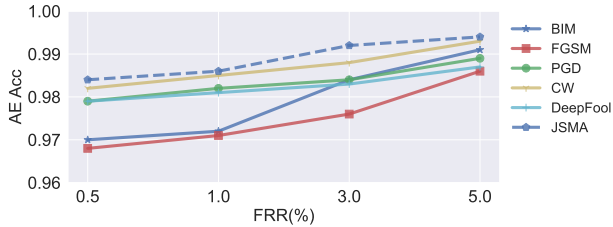


Figure 7: TRAIT performance on AudioMNIST for six white-box AE attacks, where $\epsilon = 5 \times 10^{-5}$ for the three attacks of FGSM, BIM, and PGD that can be flexibly configured.

evident that even with a preset FRR as low as 0.5%, the detection accuracy of AE on the audio dataset consistently exceeds 97% across all evaluated AE attacks. This affirms that beyond its performance in image-related tasks, TRAIT demonstrates remarkable detection proficiency in a distinct audio modality.

5.2 Textual

Setup. The textual dataset employed in this study belongs to the Stanford sentiment treebank (SST) [70], a sentiment analysis dataset publicly released by Stanford University. This dataset primarily revolves around sentiment categorization within movie reviews. SST-2, a subset of SST, focuses on binary categorization (positive or negative) and encompasses a total of 10,000 samples or sentences. Our experimentation involved training the SST-2 dataset using the BERT [19] model. We consider four mainstream textual AE attacks: Projected Word-Wise Substitution (PWWS) [61], TextBugger [40], HotFlip [21], UAT [77]. Note that PWWS, HotFlip, and UAT are white-box attacks and TextBugger is a black-box attack. Each attack is detailed in Appendix A.

Results. The BERT model was trained for 10 epochs on the SST-2 dataset, yielding a final epoch model deployed as the target model with a classification accuracy of 92.43%. Additionally, the encoder embedding dimension is set to 6.



Figure 8: TRAIT performance on SST-2 against four textual AE attacks. The target model is BERT.

These attacks were implemented using OpenAttack⁴ by utilizing 1000 randomly chosen benign text samples. As depicted in Figure 8, we configured the FRR to 1%, 3%, and 5% for each of these four textual adversarial attack methods. The results illustrate TRAIT’s exceptional detection performance against all four AE attacks, irrespective of white-box or black-box settings. Notably, the detection accuracy remains consistently above 97% even at a minimal 1% preset FRR. With a slightly higher tolerance of 3% FRR,

4. <https://github.com/thunlp/OpenAttack>

the detection accuracy surpasses 98.6% across all AE attacks. This validation underscores TRAIT’s versatility in the textual modality, demonstrating its high efficacy in identifying and capturing textual AEs.

6 NON-CLASSIFICATION TASKS

6.1 Time Series based Forecasting

Time series forecasting is crucial in applications such as environmental parameters e.g., temperature, humidity, forecasting, stock market prediction, credit scoring, energy estimation, and traffic flow forecasting.

Setup. In line with [15], we utilized the New Zealand Land Temperatures dataset, a subset of Earth Surface Temperature Data along with a Bayesian LSTM model architecture. This dataset captures real-world surface temperature data. Similar to the approach in [15], the dataset was partitioned into 1,459 training samples, 365 validation samples, and 100 test samples, each comprising 8 features—multivariate time-series. The input setup involved a three-step configuration for generating a one-step forecasting prediction. As for model architecture, we consider a 1-layer Bayesian LSTM, aligned with the architecture utilized in [15].

Table 2: TRAIT detection performance of multivariate time-series temperature forecasting.

AE Attack Method	Preset FRR(%)	AE Acc(%)
FGSM ($\epsilon = 0.2$)	1	96.47
	3	96.85
	5	98.23
BIM ($\epsilon = 0.2$)	1	95.46
	3	96.07
	5	96.17

Results. We performed training for 500 epochs, and the model from the final epoch, which achieved a mean squared error of 0.0033, serves as the target model. Similar to [15], our focus lies on targeted attacks, which hold more significance in forecasting tasks due to the attacker’s ability to set desired targeted values flexibly.

The AE attacks—using the implementation of [15]⁵—of BIM and FGSM are evaluated. As seen in Table 2, TRAIT remains highly effective against the regression task, where a higher than 95% detection accuracy is demonstrated even conditioned on a small FRR of 1%. Note that non-classification tasks are often more challenging in the field of AE countering and much less explored compared to classification tasks. In addition, the results reaffirm that the TRAIT is independent of the underlying model architecture, by noting the LSTM is a sequential model.

6.2 Image based Age Estimation

Setup. We use the APPA-REAL face dataset that is for the regression task of estimating age [3]. APPA-REAL consists of 7,591 face images, where each image is annotated with real age and appearance age. Here we consider the real age when training the model. The dataset is split into 4,113 training images, 1,500 validation images and 1,978 test images. The image size is $224 \times 224 \times 3$. The model architecture is ResNeXt50 [84].

5. <https://github.com/ProfiterolePuff/nvita>



Figure 9: TRAIT detection performance against image based age estimation.

Results. For the above time series regression, we have used targeted attacks. Now we consider the use of untargeted attacks. The age range is between 0.0 and 100.0. To ensure that the AE preserves the semantics of the benign example, the attack boundary is set within $\pm 4\%$, that is ± 4 years of the predicted age given the benign image. We randomly selected 1,200 benign examples to create AEs with four attacks: FGSM, BIM, PGD, and DeepFool. We performed 60 epochs of training, and the model for the last epoch acting as the target model exhibits a mean square error of 4.76.

The results are shown in Figure 9. The detection accuracy is no less than 96% even when the FRR is predetermined as small as 1%. When a higher FRR is tolerable, the detection accuracy can be further improved. There are three implications. First, the TRAIT is versatile to regression tasks other than classification. Second, the TRAIT is universal to data types/modalities e.g., time-series data and image data. Third, the TRAIT is effective in not only targeted but also non-targeted attacks under regression tasks.

7 ADAPTIVE ATTACK

There are many possible strategies for implementing different kinds of adaptive attacks. Exhausting them is out of the scope of this work, offering interesting future work. For our considered adaptive attack, we assume the attacker has the *same access* to all IMs as the defender does, which is essentially out of the capability of an attacker in practice to evaluate the *worst case* of TRAIT under the strongest adaptive attack. In this context, the attacker adds a regularization constraint when crafting AEs to enforce that the loss trajectory of the AE through the course of IMs is the same (or very similar) as the trajectory of its benign example counterpart. Generally, the attacker tries to make the trajectory of AE and benign examples similar by setting a distance threshold (smaller distance, higher trajectory similarity). This objective is formulated as:

$$\begin{aligned} \min_{x_{\text{adv}}} \quad & \mathcal{L}_{\text{adv}}(x_{\text{adv}}, y) + \lambda \cdot \text{Dist}_T(\mathbb{T}(x_{\text{adv}}), \mathbb{T}(x)) \\ \text{s.t.} \quad & \|x_{\text{adv}} - x\|_p \leq \epsilon, \end{aligned} \quad (1)$$

where $\mathcal{L}_{\text{adv}}(x_{\text{adv}}, y)$ denotes the adversarial loss, which can be a classification loss, e.g., cross-entropy loss. $\|x_{\text{adv}} - x\|_p \leq \epsilon$ denotes the perturbation constraint between the AE x_{adv} and the benign sample x , where p is usually ∞ . Note this is a common constraint used in AE crafting to retain visual imperceptibility.

\mathbb{T} denotes the extraction of synthetic loss values for all IMs, which can be expressed as:

$$\mathbb{T}(x) = [\mathcal{L}_1(x), \mathcal{L}_2(x), \dots, \mathcal{L}_{(K-1)}(x)], \quad (2)$$

where $\mathcal{L}_k(x)$ denotes the synthetic cross-entropy loss of the input sample x between the first k IM and the final model, i.e. $\mathcal{L}_k(x) = \text{Loss}(f_k(x), f_K(x))$. K denotes the number of all saved IMs—note that K_{th} IM is essentially the final model. $f_k(x)$ denotes the softmax output of the input sample x at the k_{th} IM.

Dist_T constrains the trajectory distance between the benign examples and its corresponding AE through e.g., L_2 norm, which is expressed as:

$$\text{Dist}_T(\mathcal{L}(x'), \mathcal{L}(x)) = \frac{\sum_{k=1}^K (\mathcal{L}(x'_k) - \mathcal{L}(x_k))^2 - \text{Dist}_T^{\min}}{\text{Dist}_T^{\max} - \text{Dist}_T^{\min}}. \quad (3)$$

In this formula, Dist_T^{\max} and Dist_T^{\min} denote the maximum and minimum values of the distance function $\text{Dist}_T(\mathcal{L}(x'), \mathcal{L}(x))$, respectively, used for normalization.

In Eq. 1, λ (1.0 is used) is the regularization factor that controls the weight of the AEs and benign examples of similarity terms in the total loss. Eq. 1 sets two main goals that an attacker considers when generating AEs: misleading the final model to misclassify (the first loss term) and generating AEs with low trajectory distance to the benign example (the second L_2 regularising constraint term) to adaptively evade TRAIT, while satisfying the perturbation constraint in Eq. 1.

By increasing the trajectory similarity, the attacker expects to evade the TRAIT detection. We use ResNet18+CIFAR10 and FGSM AE method for experiments. On the one hand, by checking the trajectory of the AE and benign samples, as shown in Figure 10 (b), they are indeed almost overlapped visually when greatly enforcing the similarity. On the other hand, in the case shown in Figure 10 (b), the success rate of crafting an AE substantially drops to only 3.3% by setting the distance threshold to 0.19 (in comparison, the success rate of AE is 76% with a distance threshold of 0.52). Nonetheless, our TRAIT still exhibits high detection accuracy of up to 95.20% with an online FRR of 2.44%. The reason is that the AE trajectory is still discernible (though small) from its benign example counterpart, especially in early epochs, which our innovative TRAIT can still capture.

As accessing the defender’s IMs is almost impossible in practice, we further consider a scenario where the attacker can train those IMs, namely surrogate IMs, by accessing the training dataset and knowledge of exact model/training parameters—such assumptions are essentially still strong as well. Then the attacker crafts the AEs following the procedure above but on the surrogate IMs. As shown in Figure 10 (c), the AE trajectory becomes more discernible than those crafted upon the defender’s IMs, which is under expectation. For those AEs, by setting the same distance threshold of 0.19 when crafting AEs, the detection rate of TRAIT now exceeds 99% with an online 1.4% FRR.

In summary, through the considered adaptive attacks, an attacker is able to craft AEs that share a similar trajectory with their benign counterparts but sacrifice a very low success rate. Even for those successful AEs, the TRAIT still maintains a high detection performance.

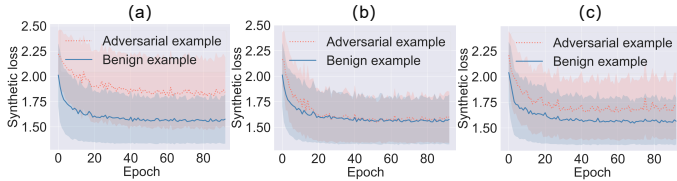


Figure 10: Comparison of trajectory overlap (a) without adaptive attack, and with adaptive by (b) using defender’s IMs and (c) surrogate IMs.

8 SCALABILITY

We demonstrate the TRAIT scalability regarding typical DL models (e.g., ResNet) and large models (e.g., pretrained natural language model). The former model is normally trained for a specific task. The latter first trains a foundation model and then fine-tunes it to downstream tasks.

8.1 Typical DL Model

The IMs need to be stored. Even though it is acceptable to take the trade-off between the memory and model security robustness, especially for security sensitive applications e.g., facial recognition and malware detection, it is still preferable to reduce the memory overhead to store these IMs.

Table 3: TRAIT detection performance when only early epochs (i.e., the first 10, 20 and 30) synthetic losses are used (CIFAR10+ResNet18).

AE Attack Method	Preset FRR(%)	AE Acc(%)			
		Epochs=10	Epochs=20	Epochs=30	Epochs=104
FGSM	1	95.88	96.11	96.42	98.31
	3	96.79	97.32	97.37	98.80
	5	97.17	97.41	97.55	99.38
PGD	1	95.07	95.18	95.80	97.45
	3	95.89	96.04	96.08	98.01
	5	96.93	97.13	97.36	98.33

The disparity in trajectory imprint between benign and adversarial examples is notably prominent in the initial epochs, as depicted in Figures 2 and 3. So we may solely rely on these early epoch imprints to capture AEs, which could potentially be sufficient. This approach could substantially reduce stored IMs and, thus the memory overhead.

To validate this hypothesis, we computed the synthetic loss using only the first 10, 20 and 30 IMs (each IM corresponds to one epoch), respectively, and the final model for the CIFAR10+ResNet18 combination. Specifically, PGD and FGSM were evaluated with $\epsilon = 8/255$. The results are presented in Table 3. Notably, when the number of IMs is limited to as small as 10, there is only a marginal drop in TRAIT detection accuracy (e.g., less than 2.5%) for both FGSM and PGD in comparison to the results in Table 1 (also copied into the last column where number of epochs is 104) at preset FRR values of 1%, 3%, 5%, respectively. This reduction in memory size is approximately 90%. Remarkably, the detection accuracy remains more than 95.0% even at a minimal 1% FRR.

In addition to reducing the number of IMs, further reductions in the model size of each IM can be achieved through various post-training DL model compression techniques, including quantization, weight clustering, and pruning. These techniques, capable of significantly reducing

model size while preserving performance, are supported by leading commercial machine learning frameworks such as TensorFlow-Lite and PyTorch Mobile [22], [27], [45]. Importantly, each of these compression operations can be separately applied through corresponding APIs, or *combined for more comprehensive compression*. Furthermore, as consecutive IMs share similarities, weight sharing across consecutive IMs might be feasible.

8.2 Large Model

As for large pretrained language models, they can have hundreds of millions of parameters (e.g., RoBERTa [42], with a parameter count of about 120 million). These models are trained for general tasks and then can be customized to downstream tasks. It is absolutely unwise to fine-tune the entire model for downstream tasks, where parameter-efficient fine-tuning (PEFT) methods [31] such as Low-Rank Adaptation (LoRA) [34] are often leveraged by fine-tuning only a small fraction of (additional) model parameters to save computational overhead.

We use LoRA to fine-tune RoBERTa which is one of the large language models. The LoRA adds a small set of trainable parameters (665,858 parameters) while freezing the entire RoBERTa with 125,313,028 parameters. The fine-tuning parameters account for only 0.53% of all parameters. We fine-tune 10 epochs using the SST-2 [70] dataset for utterance sentiment classification, and the final CDA is 92.44%. For PWWS [61] and HotFlip [21] attacks, the detection accuracy is 98.55% and 98.24% at preset FRR of 1%, respectively. The additional storage memory overhead by incorporating TRAIT is only about 5.3% ($0.53\% \times 10$) considering 10 epochs. This fully demonstrates the scalability of TRAIT on large models.

9 DISCUSSION

9.1 Component Ablation Study

TRAIT component’s functionality has been qualitatively justified in subsection 2.2 (particularly visualized in Figure 4), we now quantify core components functionality.

The CIFAR10 dataset with ResNet18 is used to assess the effectiveness of each component of TRAIT. Specifically, we crafted 2,000 AEs using the BIM method ($\epsilon = 8/255$) and evaluated TRAIT’s performance under three different settings: i) removing noise reduction and FFT (used for spectrum transformation); ii) removing noise reduction; and iii) removing FFT. The performance of TRAIT under each setting is detailed in Table 4.

The results demonstrate that TRAIT fails to achieve satisfactory performance if any component is omitted. With a preset 1% FRR, removing the noise reduction component results in a decrease in detection accuracy from 97.94% to 87.43%, representing a drop of approximately 10%. Removing the FFT or spectrum transformation causes an even more significant drop in detection accuracy, by 55%. When both FFT and noise reduction are excluded, the detection accuracy plummets to just 9.32%, rendering it useless.

These quantifications underscore the importance of TRAIT’s innovative component design, particularly the incorporation of spectrum transformation and noise reduc-

tion, with spectrum transformation being the most critical component.

Table 4: TRAIT’s components ablation study.

Removed Component	Preset FRR(%)	AE Acc(%)
Noise reduction	1	87.43
FFT (Spectrum Transformation)	1	43.20
Noise reduction + FFT	1	9.32
TRAIT	1	97.94

9.2 More Attack

To further demonstrate the TRAIT generality to unknown attacks, we evaluate its performance on a recent AE attack on automatic speech recognition that is SMACK [88] (USENIX 2023’)—modifying inherent speech attribute of prosody. SMACK was shown to be evasive SOTA defenses [88]. Following the SMACK setup, we evaluated TRAIT. SMACK utilizes a generative model to produce adversarial examples. The victim model is DeepSpeech 2 [5] trained on LibriSpeech [55].

We trained DeepSpeech 2 for 70 epochs and saved 70 IMs. The last epoch model is the deployed target model that has a word error rate of 10.51% in the LibriSpeech dataset. Note that SMACK generates adversarial audio using the Common Voice [7] dataset, which contains 81,085 human speech sentences, as the raw audio data. We randomly selected 500 examples from Common Voice, and the generated adversarial examples’ attack success rate on DeepSpeech 2 is 87.6%, similar to the SMACK reported attack success rate of 88.3%. *TRAIT detection accuracy for these successful adversarial audio examples is 95.74%, 96.21%, 96.76% at preset FRR of 1%, 3%, 5% respectively.*

9.3 Category Number

Here, we evaluate the TRAIT sensitivity to the number of categories in the classification tasks. The dataset of CIFAR100 with 100 classes is now used and the model of VGG16 is used. Different subsets of CIFAR100 with different numbers of categories are used for evaluations. The number is set to 20, 40, 60, and 80, respectively, and the whole dataset of 100 classes is also considered. We extensively evaluate the TRAIT with FGSM and BIM attacks, both of which were evaluated at $\epsilon = 8/255$.

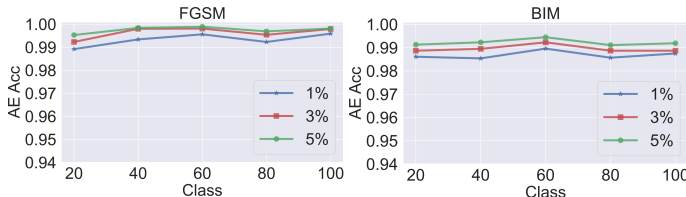


Figure 11: TRAIT is independent of the number of classes. CIFAR100 dataset is used.

The results are depicted in Figure 11. For each number of classes, we trained 130 epochs, all of which generated about 1500 adversarial examples. We preset FRR to 1%, 3% and 5%, respectively. We find that changes in the number of classes do not cause notable changes in the detection

capability of TRAIT. In other words, TRAIT is insensitive to changes in the number of classes. In addition, the AE detection accuracy is higher than 98% even given a 1% FRR, which is consistent with the results of CIFAR10 and STL10 in Table 1.

10 LATENCY OVERHEAD

Compared to the standard inference latency of the target model, TRAIT introduces additional sequential operations: loss synthesis, dimension reduction through an encoder, and assessment of adversarial behavior via Deep-SVDD. Importantly, the inference operation of IMs compared with the target model is not sequential, allowing for parallel execution. Thus, we quantify the time overhead for each sequential component using the VGG16 model and the CIFAR10 dataset, with 1000 examples dedicated to validation.

The average time overhead per image for target/IM model inference, loss synthesis, dimension reduction, and adversarial behavior detection through Deep SVDD is 0.47ms, 0.004ms, 0.06ms, and 0.07ms, respectively. Notably, all computations are conducted on a single CPU. Given that IMs operate in parallel with the target model, the additional latency introduced by TRAIT including loss synthesis, dimension reduction, and adversarial behavior detection, is approximately 28.5% (0.136ms to 0.47ms), which remains completely acceptable for enhanced security benefits.

10.1 More Complicated Dataset

For the image datasets, We have extensively evaluated CIFAR10 and STL10 for comprehensive validations in section 4. In subsection 9.3, we have also evaluated CIFAR100. We now further evaluate on a more complicated dataset, TinyImageNet [38]. We trained 200 epochs on ResNet18, with a 67.37% CDA. We used only the first 30 IMs for TRAIT, which is to further validate the scalability as in subsection 8.1. TRAIT detection performance against FGSM and PGD is shown in Table 5. TRAIT has a detection accuracy of not less than 96%, which shows that TRAIT still maintains an excellent performance on more complicated datasets, even when only using a small number of IMs. As TinyImageNet has 200 classes, this also validates the TRAIT is insensitive to the number of categories.

Table 5: TRAIT detection performance on TinyImageNet.

AE Attack Method	Preset FRR(%)	AE Acc(%)
FGSM ($\epsilon = 8/255$)	1	96.60
	3	97.45
	5	97.70
BIM ($\epsilon = 8/255$)	1	96.15
	3	96.54
	5	97.12

10.2 Imprint Types

In addition to the universal metric of loss, we expect that the exploration of alternative imprints such as latent representation and softmax may exhibit more pronounced discrepancies between adversarial and benign examples. These imprints, capturing finer-grained information than the loss metric, offer a promising avenue for analysis.

However, they often lack universality; for instance, while softmax is prevalent in classification tasks, its applicability to non-classification tasks remains limited. Moreover, these alternative imprints typically exhibit higher dimensionality compared to the loss. Consider a scenario involving facial recognition having 10,000 identities with 100 IMs: the dimensionality of the softmax imprint to the encoder amounts to $10,000 \times 100$, a significantly higher dimension than the 1×100 dimensionality of the loss imprint. Nevertheless, exploring alternative imprints holds merit, especially if they offer superior discriminative capabilities in *specific* applications.

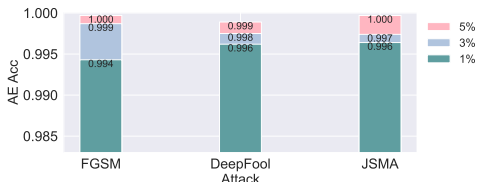


Figure 12: TRAIT detection performance when the softmax is used as an imprint (CIFAR10+ResNet18).

Softmax Imprint: To assess the efficacy of employing softmax as an imprint, we evaluated the performance of TRAIT using CIFAR10 and ResNet18. Notably, CIFAR10 has ten categories, rendering the softmax imprint to the LSTM-autoencoder akin to a 10-channel/feature time-series signal. The evaluation settings align with those detailed in section 4. For adversarial attacks, we employed FGSM ($\epsilon = 8/255$), DeepFool, and JSMA. The outcomes, illustrated in Figure 12, demonstrate an enhanced detection accuracy while maintaining a consistent FRR. For instance, the detection accuracy against FGSM improved from 98.31% (as indicated in Table 1) to 99.40% given a 1% FRR. This improvement underscores the effectiveness of leveraging softmax directly, which encodes finer-grained information and better captures adversarial examples.

10.3 Loss Synthesis

When synthesizing loss, all previous experiments use each of IMs softmax and the target model’s softmax for computing the loss. Here we explore other loss synthesis means. Specifically, we synthesize the loss using the softmax of every two consecutive IMs. The detection accuracy is summarized in Table 7 in Appendix, where three AE attacks are evaluated and all the experimental settings are the same as section 4 (CIFAR10+VGG16). The performance using loss synthesized upon two consecutive IMs (second last column) is slightly lower than the performance using loss synthesized upon softmax of each IM and the target model (last column replicated from Table 1 to ease comparison). Nonetheless, the detection accuracy is still no less than 98% even given a 1% FRR.

10.4 Comparison

This work mainly aims to *uncover a new paradigm of understanding the temporal traces left by adversarial attacks*, which is later demonstrated to be highly effective in capturing such attacks. Considering that TRAIT does not necessitate

prior knowledge of AE attacks, falling within the class of unsupervised AE detection, we conducted a comparative analysis of TRAIT against two unsupervised AE detection methods. Specifically, they are NIC [46] (NDSS ’2019), and ContraNet [87] (NDSS ’2022), which we reproduced these two works.

We employed five attack methods, namely FGSM, PGD, JSMA, DeepFool and Boundary attack, for comparative validation. For FGSM, PGD, the ϵ was set to $8/255$, other experimental settings are the same as in Table 1. The comparison results are summarized in Figure 13, and the preset FRR was set to 5%. This relatively high FRR of 5%—TRAIT still performs well given a 1% FRR—is to align with settings of NIC and ContraNet, their detection accuracy is even worse when a lower FRR is set. It is worth mentioning that TRAIT, NIC and ContraNet have excellent performance in detecting PGD AEs with accuracies of 98.33%, 96.33% and 98.40%, respectively. However, NIC and ContraNet are much lower than TRAIT in detecting the other four AE methods.

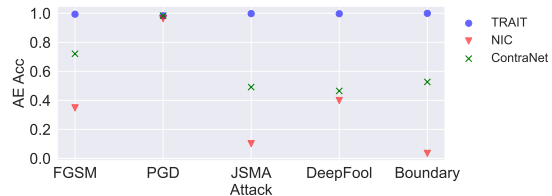


Figure 13: Comparison of TRAIT with NIC and ContraNet.

11 RELATED WORK

To counter AE attacks, three main approaches can be leveraged (detailed in Appendix B). The first approach modifies the training procedure or the underlying model architecture [28], [50], [60], [65], represented by adversarial training [50], [60], [65]. The second approach performs input transformation such as such as JPEG compression [20], [44], bit reduction [29], [86], pixel deflection [59], or employing random transformations [82] to eliminate the attack effect. The third approach that is mostly studied is to detect AEs [17], [23], [33], [39], [47], [56], [73].

Limitations. These countermeasures all suffer one or more shortcomings. First, the model/training modification and input transformation often suffer an accuracy trade-off to benign examples [52], [66], [87], [95]. Second, it is noted that the majority of these defenses are designed to counter AE in the imaging modality explicitly or inexplicitly. They are facing challenges to be adapting to other data modalities, for example, those reconstruction based and input transformation based [33], [79], [80], [86], [87]. Third, the majority are devised for classification tasks [46], [87], [94], they might be inapplicable to other tasks e.g., regression. Last, some of them require modifying the training process or model architecture [46], [66], [94], [95], which usually comes with a substantially increased computational overhead and a trade-off of the accuracy to benign examples. As for detection methods, they can suffer a high FRR, for example, ContraNet sets a 5% FRR for AE detection accuracy evaluations and it witnesses a detection performance drop

when this tolerable FRR is set to be a bit lower [87]. In other words, it is extremely challenging to have a high detection accuracy e.g., 90% under the constraint of a small FRR e.g., 1%, as also evidenced in Figure 13.

Notably, numerous studies depend on observed AEs, particularly those utilizing adversarial training and detection-based methods, making them intrinsically susceptible to unseen AE attacks and especially adaptive attacks [4], [67]. Thus, it becomes crucial to develop a defense mechanism that does not rely on prior knowledge of specific attacks.

Spatial Imprint VS Temporal Imprint. All existing AE detection methods rely on static or spatial only adversarial imprints of the target underlying model or focus on adversarial training on the underlying model. They all overlook the information easily available from temporal trajectory imprints. We are the first to explore a new dimension: the temporal information or historical imprints of the target underlying model in the particular spectrum domain that are distinctly traceable.

12 CONCLUSION

This study has unveiled the previously elusive temporal trajectory imprinted by AE attacks, introducing a new and fresh perspective in understanding and combating adversarial behavior. Through the innovative application of synthetic loss as a universal metric, the proposed TRAIT, adeptly identifies and isolates AEs in a diverse range of scenarios. This method stands out for its ability to encapsulate the adversarial temporal trajectory in a comprehensive and effective manner. TRAIT's prowess has been validated across a battery of experiments, successfully countering up to 12 different types of AE attacks and strong adaptive attacks without any attacking foreknowledge. Its robustness is further underscored by its consistent performance across various model architectures, including but not limited to ResNet, ResNeXt, VGG, AudioNet, BERT, and DeepSpeech. Moreover, TRAIT has demonstrated its versatility by performing equally well across different data modalities (such as images, audio, and text), task categories (including both classification and regression), and datasets.

REFERENCES

- [1] Hadi Abdullah, Kevin Warren, Vincent Bindschaedler, Nicolas Papernot, and Patrick Traynor. Sok: The faults in our ASRs: An overview of attacks against automatic speech recognition and speaker identification systems. In *IEEE Symposium on Security and Privacy (SP)*, pages 730–747. IEEE, 2021.
- [2] Ahmed Abusnaina, Yuhang Wu, Sunpreet Arora, Yizhen Wang, Fei Wang, Hao Yang, and David Mohaisen. Adversarial example detection using latent neighborhood graph. In *Proceedings of the IEEE/CVF International Conference on Computer Vision*, pages 7687–7696, 2021.
- [3] Eirikur Agustsson, Radu Timofte, Sergio Escalera, Xavier Baro, Isabelle Guyon, and Rasmus Rothe. Apparent and real age estimation in still images with deep residual regressors on appa-real database. In *2017 12th IEEE International Conference on Automatic Face & Gesture Recognition (FG 2017)*, pages 87–94. IEEE, 2017.
- [4] Ahmed Aldahdooh, Wassim Hamidouche, Sid Ahmed Fezza, and Olivier Déforges. Adversarial example detection for dnn models: A review and experimental comparison. *Artificial Intelligence Review*, 55(6):4403–4462, 2022.
- [5] Dario Amodei, Sundaram Ananthanarayanan, Rishita Anubhai, Jingliang Bai, Eric Battenberg, Carl Case, Jared Casper, Bryan Catanzaro, Qiang Cheng, Guoliang Chen, et al. Deep speech 2: End-to-end speech recognition in english and mandarin. In *International Conference on Machine Learning*, pages 173–182. PMLR, 2016.
- [6] Shengwei An, Yuan Yao, Qiuling Xu, Shiqing Ma, Guan hong Tao, Siyuan Cheng, Kaiyuan Zhang, Yingqi Liu, Guangyu Shen, Ian Kelk, et al. Imu: Physical impersonating attack for face recognition system with natural style changes. In *2023 IEEE Symposium on Security and Privacy (SP)*, pages 899–916. IEEE Computer Society, 2023.
- [7] Rosana Ardila, Megan Branson, Kelly Davis, Michael Henretty, Michael Kohler, Josh Meyer, Reuben Morais, Lindsay Saunders, Francis M Tyers, and Gregor Weber. Common voice: A massively-multilingual speech corpus. *arXiv preprint arXiv:1912.06670*, 2019.
- [8] Emilio Rafael Balda, Arash Behboodi, and Rudolf Mathar. Perturbation analysis of learning algorithms: Generation of adversarial examples from classification to regression. *IEEE Transactions on Signal Processing*, 67(23):6078–6091, 2019.
- [9] Sören Becker, Marcel Ackermann, Sebastian Lapuschkin, Klaus-Robert Müller, and Wojciech Samek. Interpreting and explaining deep neural networks for classification of audio signals. *CoRR*, abs/1807.03418, 2018.
- [10] Mazal Bethany, Andrew Seong, Samuel Henrique Silva, Nicole Beebe, Nishant Vishwamitra, and Peyman Najafirad. Towards targeted obfuscation of adversarial unsafe images using reconstruction and counterfactual super region attribution explainability. In *USENIX Security Symposium*, pages 643–660, 2023.
- [11] Wieland Brendel, Jonas Rauber, and Matthias Bethge. Decision-based adversarial attacks: Reliable attacks against black-box machine learning models. *arXiv preprint arXiv:1712.04248*, 2017.
- [12] Xiaoyu Cao, Jinyuan Jia, Zaixi Zhang, and Neil Zhenqiang Gong. Fedrecover: Recovering from poisoning attacks in federated learning using historical information. In *2023 IEEE Symposium on Security and Privacy (SP)*, pages 1366–1383. IEEE, 2023.
- [13] Nicholas Carlini and David Wagner. Towards evaluating the robustness of neural networks. In *2017 IEEE Symposium on Security and Privacy (S&P)*, pages 39–57. IEEE, 2017.
- [14] Yanzuo Chen, Yuanyuan Yuan, and Shuai Wang. OBSan: An out-of-bound sanitizer to harden DNN executables. In *Network and Distributed System Security Symposium (NDSS)*, 2023.
- [15] Zeyu Chen, Katharina Dost, Xuan Zhu, Xinglong Chang, Gillian Dobbie, and Jörg Wicker. Targeted attacks on time series forecasting. In *Pacific-Asia Conference on Knowledge Discovery and Data Mining*, pages 314–327. Springer, 2023.
- [16] Adam Coates, Andrew Ng, and Honglak Lee. An analysis of single-layer networks in unsupervised feature learning. In *Proceedings of the fourteenth international conference on artificial intelligence and statistics*, pages 215–223. JMLR Workshop and Conference Proceedings, 2011.
- [17] Gilad Cohen, Guillermo Sapiro, and Raja Giryes. Detecting adversarial samples using influence functions and nearest neighbors. In *Proceedings of the IEEE/CVF Conference on Computer Vision and Pattern Recognition*, pages 14453–14462, 2020.
- [18] Hanjun Dai, Hui Li, Tian Tian, Xin Huang, Lin Wang, Jun Zhu, and Le Song. Adversarial attack on graph structured data. In *International Conference on Machine Learning*, pages 1115–1124. PMLR, 2018.
- [19] Jacob Devlin, Ming-Wei Chang, Kenton Lee, and Kristina Toutanova. Bert: Pre-training of deep bidirectional transformers for language understanding. *arXiv preprint arXiv:1810.04805*, 2018.
- [20] Gintare Karolina Dziugaite, Zoubin Ghahramani, and Daniel M Roy. A study of the effect of jpg compression on adversarial images. *arXiv preprint arXiv:1608.00853*, 2016.
- [21] Javid Ebrahimi, Anyi Rao, Daniel Lowd, and Dejing Dou. Hotflip: White-box adversarial examples for text classification. In *Proceedings of the 56th Annual Meeting of the Association for Computational Linguistics*, pages 31–36, 2018.
- [22] Facebook. End-to-end workflow from training to deployment for ios and android mobile devices, January 2021.
- [23] Reuben Feinman, Ryan R Curtin, Saurabh Shintre, and Andrew B Gardner. Detecting adversarial samples from artifacts. *arXiv preprint arXiv:1703.00410*, 2017.
- [24] Ji Gao, Jack Lanchantin, Mary Lou Soffa, and Yanjun Qi. Black-box generation of adversarial text sequences to evade deep learning

- classifiers. In *2018 IEEE Security and Privacy Workshops (SPW)*, pages 50–56. IEEE, 2018.
- [25] Yansong Gao, Bao Gia Doan, Zhi Zhang, Siqi Ma, Anmin Fu, Surya Nepal, and Hyoungshick Kim. Backdoor attacks and countermeasures on deep learning: a comprehensive review. *arXiv preprint arXiv:2007.10760*, 2020.
- [26] Ian J Goodfellow, Jonathon Shlens, and Christian Szegedy. Explaining and harnessing adversarial examples. *arXiv preprint arXiv:1412.6572*, 2014.
- [27] Google. Deploy machine learning models on mobile and edge devices, January 2021.
- [28] Kathrin Grosse, Praveen Manoharan, Nicolas Papernot, Michael Backes, and Patrick McDaniel. On the (statistical) detection of adversarial examples. *arXiv preprint arXiv:1702.06280*, 2017.
- [29] Chuan Guo, Mayank Rana, Moustapha Cisse, and Laurens van der Maaten. Countering adversarial images using input transformations. *arXiv preprint arXiv:1711.00117*, 2017.
- [30] Sicong Han, Chenhao Lin, Chao Shen, Qian Wang, and Xiaohong Guan. Interpreting adversarial examples in deep learning: A review. *ACM Computing Surveys*, 2023.
- [31] Zeyu Han, Chao Gao, Jinyang Liu, Sai Qian Zhang, et al. Parameter-efficient fine-tuning for large models: A comprehensive survey. *arXiv preprint arXiv:2403.14608*, 2024.
- [32] Kaiming He, Xiangyu Zhang, Shaoqing Ren, and Jian Sun. Deep residual learning for image recognition. In *Proc. CVPR*, pages 770–778, 2016.
- [33] Chih-Hui Ho and Nuno Vasconcelos. DISCO: Adversarial defense with local implicit functions. *Advances in Neural Information Processing Systems*, 35:23818–23837, 2022.
- [34] Edward J Hu, Yelong Shen, Phillip Wallis, Zeyuan Allen-Zhu, Yuanzhi Li, Shean Wang, Lu Wang, and Weizhu Chen. Lora: Low-rank adaptation of large language models. *arXiv preprint arXiv:2106.09685*, 2021.
- [35] Shehzeen Hussain, Paarth Neekhara, Shlomo Dubnov, Julian McAuley, and Farinaz Koushanfar. WaveGuard: Understanding and mitigating audio adversarial examples. In *USENIX Security Symposium*, pages 2273–2290, 2021.
- [36] Alex Krizhevsky, Geoffrey Hinton, et al. Learning multiple layers of features from tiny images. 2009.
- [37] Alexey Kurakin, Ian J Goodfellow, and Samy Bengio. Adversarial examples in the physical world. In *Artificial Intelligence Safety and Security*, pages 99–112. Chapman and Hall/CRC, 2018.
- [38] Ya Le and Xuan Yang. Tiny imagenet visual recognition challenge. *CS 231N*, 7(7):3, 2015.
- [39] Kimin Lee, Kibok Lee, Honglak Lee, and Jinwoo Shin. A simple unified framework for detecting out-of-distribution samples and adversarial attacks. *Advances in Neural Information Processing Systems*, 31, 2018.
- [40] Jinfeng Li, Shouling Ji, Tianyu Du, Bo Li, and Ting Wang. Textbugger: Generating adversarial text against real-world applications. *Network and Distributed System Security Symposium*, 2019.
- [41] Yige Li, Xixiang Lyu, Nodens Koren, Lingjuan Lyu, Bo Li, and Xingjun Ma. Anti-backdoor learning: Training clean models on poisoned data. *Proc. NIPS*, 34:14900–14912, 2021.
- [42] Yinhan Liu, Myle Ott, Naman Goyal, Jingfei Du, Mandar Joshi, Danqi Chen, Omer Levy, Mike Lewis, Luke Zettlemoyer, and Veselin Stoyanov. Roberta: A robustly optimized bert pretraining approach. *arXiv preprint arXiv:1907.11692*, 2019.
- [43] Yiyong Liu, Zhengyu Zhao, Michael Backes, and Yang Zhang. Membership inference attacks by exploiting loss trajectory. In *Proceedings of the 2022 ACM SIGSAC Conference on Computer and Communications Security*, pages 2085–2098, 2022.
- [44] Zihao Liu, Qi Liu, Tao Liu, Nuo Xu, Xue Lin, Yanzhi Wang, and Wujie Wen. Feature distillation: Dnn-oriented jpeg compression against adversarial examples. In *2019 IEEE/CVF Conference on Computer Vision and Pattern Recognition (CVPR)*, pages 860–868. IEEE, 2019.
- [45] Hua Ma, Huming Qiu, Yansong Gao, Zhi Zhang, Alsharif Abuadbba, Minhui Xue, Anmin Fu, Jiliang Zhang, Said F Al-Sarawi, and Derek Abbott. Quantization backdoors to deep learning commercial frameworks. *IEEE Transactions on Dependable and Secure Computing*, 2023.
- [46] Shiqing Ma, Yingqi Liu, Guanhong Tao, Wen-Chuan Lee, and Xiangyu Zhang. Nic: Detecting adversarial samples with neural network invariant checking. In *26th Annual Network And Distributed System Security Symposium (NDSS 2019)*. Internet Soc, 2019.
- [47] Xingjun Ma, Bo Li, Yisen Wang, Sarah M Erfani, Sudanthi Wijewickrema, Grant Schoenebeck, Dawn Song, Michael E Houle, and James Bailey. Characterizing adversarial subspaces using local intrinsic dimensionality. In *International Conference on Learning Representations (ICLR)*, 2018.
- [48] Gabriel Resende Machado, Eugênio Silva, and Ronaldo Ribeiro Goldschmidt. Adversarial machine learning in image classification: A survey toward the defender’s perspective. *ACM Computing Surveys (CSUR)*, 55(1):1–38, 2021.
- [49] Aleksander Madry, Aleksandar Makelov, Ludwig Schmidt, Dimitris Tsipras, and Adrian Vladu. Towards deep learning models resistant to adversarial attacks. *arXiv preprint arXiv:1706.06083*, 2017.
- [50] Aleksander Madry, Aleksandar Makelov, Ludwig Schmidt, Dimitris Tsipras, and Adrian Vladu. Towards deep learning models resistant to adversarial attacks. In *International Conference on Learning Representations*, 2018.
- [51] Filippo Menczer, David Crandall, Yong-Yeol Ahn, and Apu Kapadia. Addressing the harms of AI-generated inauthentic content. *Nature Machine Intelligence*, 5(7):679–680, 2023.
- [52] Dongyu Meng and Hao Chen. Magnet: a two-pronged defense against adversarial examples. In *Proceedings of the 2017 ACM SIGSAC Conference on Computer and Communications Security*, pages 135–147, 2017.
- [53] Jaron Mink, Harjot Kaur, Juliane Schmäser, Sascha Fahl, and Yasemin Acar. “security is not my field, i’m a stats guy”: A qualitative root cause analysis of barriers to adversarial machine learning defenses in industry. In *In 32nd USENIX Security Symposium*, 2023.
- [54] Seyed-Mohsen Moosavi-Dezfooli, Alhussein Fawzi, and Pascal Frossard. Deepfool: a simple and accurate method to fool deep neural networks. In *Proceedings of the IEEE Conference on Computer Vision and Pattern Recognition*, pages 2574–2582, 2016.
- [55] Vassil Panayotov, Guoguo Chen, Daniel Povey, and Sanjeev Khudanpur. Librispeech: an asr corpus based on public domain audio books. In *IEEE International Conference on Acoustics, Speech and Signal Processing (ICASSP)*, pages 5206–5210. IEEE, 2015.
- [56] Nicolas Papernot and Patrick McDaniel. Deep k-nearest neighbors: Towards confident, interpretable and robust deep learning. *arXiv preprint arXiv:1803.04765*, 2018.
- [57] Nicolas Papernot, Patrick McDaniel, Somesh Jha, Matt Fredrikson, Z Berkay Celik, and Ananthram Swami. The limitations of deep learning in adversarial settings. In *IEEE European Symposium on Security and Privacy (EuroS&P)*, pages 372–387. IEEE, 2016.
- [58] Nicolas Papernot, Patrick McDaniel, Arunesh Sinha, and Michael P Wellman. Sok: Security and privacy in machine learning. In *2018 IEEE European Symposium on Security and Privacy (EuroS&P)*, pages 399–414. IEEE, 2018.
- [59] Aaditya Prakash, Nick Moran, Solomon Garber, Antonella DiLillo, and James Storer. Deflecting adversarial attacks with pixel deflection. In *Proceedings of the IEEE Conference on Computer Vision and Pattern Recognition*, pages 8571–8580, 2018.
- [60] Rahul Rade and Seyed-Mohsen Moosavi-Dezfooli. Reducing excessive margin to achieve a better accuracy vs. robustness trade-off. In *International Conference on Learning Representations*, 2021.
- [61] Shuhuai Ren, Yihe Deng, Kun He, and Wanxiang Che. Generating natural language adversarial examples through probability weighted word saliency. In *Proceedings of the 57th Annual Meeting of the Association for Computational Linguistics*, pages 1085–1097, 2019.
- [62] Lukas Ruff, Robert Vandermeulen, Nico Goernitz, Lucas Deecke, Shoaib Ahmed Siddiqui, Alexander Binder, Emmanuel Müller, and Marius Kloft. Deep one-class classification. In *International Conference on Machine Learning*, pages 4393–4402. PMLR, 2018.
- [63] Ahmed Salem, Giovanni Cherubini, David Evans, Boris Köpf, Andrew Paverd, Anshuman Suri, Shruti Tople, and Santiago Zanella-Béguelin. Sok: Let the privacy games begin! a unified treatment of data inference privacy in machine learning. In *2023 IEEE Symposium on Security and Privacy (SP)*, pages 327–345. IEEE, 2023.
- [64] Pouya Samangouei, Maya Kabkab, and Rama Chellappa. Defensegan: Protecting classifiers against adversarial attacks using generative models. In *6th International Conference on Learning Representations, ICLR 2018*, 2018.
- [65] Vikash Sehwal, Saeed Mahloujifar, Tinashe Handina, Sihui Dai, Chong Xiang, Mung Chiang, and Prateek Mittal. Robust learning meets generative models: Can proxy distributions improve adversarial robustness? In *International Conference on Learning Representations*, 2021.

- [66] Shawn Shan, Emily Wenger, Bolun Wang, Bo Li, Haitao Zheng, and Ben Y Zhao. Gotta catch'em all: Using honeypots to catch adversarial attacks on neural networks. In *Proceedings of the 2020 ACM SIGSAC Conference on Computer and Communications Security*, pages 67–83, 2020.
- [67] Ryan Sheatsley, Blaine Hoak, Eric Pauley, and Patrick McDaniel. The space of adversarial strategies. In *32nd USENIX Security Symposium (USENIX Security 23)*, pages 3745–3761, Anaheim, CA, August 2023. USENIX Association.
- [68] Iliia Shumailov, Yiren Zhao, Robert Mullins, and Ross Anderson. Towards certifiable adversarial sample detection. In *Proceedings of the 13th ACM Workshop on Artificial Intelligence and Security*, pages 13–24, 2020.
- [69] Karen Simonyan and Andrew Zisserman. Very deep convolutional networks for large-scale image recognition. *arXiv preprint arXiv:1409.1556*, 2014.
- [70] Richard Socher, Alex Perelygin, Jean Wu, Jason Chuang, Christopher D Manning, Andrew Y Ng, and Christopher Potts. Recursive deep models for semantic compositionality over a sentiment treebank. In *Proceedings of the 2013 Conference on Empirical Methods in Natural Language Processing*, pages 1631–1642, 2013.
- [71] Dawn Song, Kevin Eykholt, Ivan Evtimov, Earlene Fernandes, Bo Li, Amir Rahmati, Florian Tramer, Atul Prakash, and Tadayoshi Kohno. Physical adversarial examples for object detectors. In *12th USENIX Workshop on Offensive Technologies (WOOT 18)*, 2018.
- [72] Jiachen Sun, Yulong Cao, Qi Alfred Chen, and Z. Morley Mao. Towards robust LiDAR-based perception in autonomous driving: General black-box adversarial sensor attack and countermeasures. In *29th USENIX Security Symposium (USENIX Security 20)*, pages 877–894. USENIX Association, 2020.
- [73] Jan Svoboda, Jonathan Masci, Federico Monti, Michael Bronstein, and Leonidas Guibas. Peernets: Exploiting peer wisdom against adversarial attacks. In *International Conference on Learning Representations*, 2019.
- [74] Christian Szegedy, Wojciech Zaremba, Ilya Sutskever, Joan Bruna, Dumitru Erhan, Ian Goodfellow, and Rob Fergus. Intriguing properties of neural networks. *arXiv preprint arXiv:1312.6199*, 2013.
- [75] David MJ Tax and Robert PW Duin. Support vector data description. *Machine Learning*, 54:45–66, 2004.
- [76] Laurens Van der Maaten and Geoffrey Hinton. Visualizing data using t-SNE. *Journal of Machine Learning Research*, 9(11), 2008.
- [77] Eric Wallace, Shi Feng, Nikhil Kandpal, Matt Gardner, and Sameer Singh. Universal adversarial triggers for attacking and analyzing NLP. In *Proceedings of the Conference on Empirical Methods in Natural Language Processing and the International Joint Conference on Natural Language Processing (EMNLP-IJCNLP)*, 2019.
- [78] Ningfei Wang, Yunpeng Luo, Takami Sato, Kaidi Xu, and Qi Alfred Chen. Does physical adversarial example really matter to autonomous driving? towards system-level effect of adversarial object evasion attack. In *Proceedings of the IEEE/CVF International Conference on Computer Vision*, pages 4412–4423, 2023.
- [79] Yuchen Wang, Xiaoguang Li, Li Yang, Jianfeng Ma, and Hui Li. Addition: Detecting adversarial examples with image-dependent noise reduction. *IEEE Transactions on Dependable and Secure Computing*, 2023.
- [80] Chong Xiang, Saeed Mahloujifar, and Prateek Mittal. {PatchCleanser}: Certifiably robust defense against adversarial patches for any image classifier. In *USENIX Security Symposium*, pages 2065–2082, 2022.
- [81] Chong Xiang, Alexander Valtchanov, Saeed Mahloujifar, and Prateek Mittal. Objectseeker: Certifiably robust object detection against patch hiding attacks via patch-agnostic masking. In *2023 IEEE Symposium on Security and Privacy (SP)*, pages 1329–1347. IEEE, 2023.
- [82] Cihang Xie, Jianyu Wang, Zhishuai Zhang, Zhou Ren, and Alan Yuille. Mitigating adversarial effects through randomization. *arXiv preprint arXiv:1711.01991*, 2017.
- [83] Cihang Xie, Jianyu Wang, Zhishuai Zhang, Yuyin Zhou, Lingxi Xie, and Alan Yuille. Adversarial examples for semantic segmentation and object detection. In *Proceedings of the IEEE International Conference on Computer Vision*, pages 1369–1378, 2017.
- [84] Saining Xie, Ross Girshick, Piotr Dollár, Zhuowen Tu, and Kaiming He. Aggregated residual transformations for deep neural networks. In *Proceedings of the IEEE Conference on Computer Vision and Pattern Recognition*, pages 1492–1500, 2017.
- [85] Han Xu, Yao Ma, Hao-Chen Liu, Debayan Deb, Hui Liu, Ji-Liang Tang, and Anil K Jain. Adversarial attacks and defenses in images, graphs and text: A review. *International Journal of Automation and Computing*, 17:151–178, 2020.
- [86] Weilin Xu, David Evans, and Yanjun Qi. Feature squeezing: Detecting adversarial examples in deep neural networks. In *Network and Distributed System Security Symposium*, 2018.
- [87] Yijun Yang, Ruiyuan Gao, Yu Li, Qiuxia Lai, and Qiang Xu. What you see is not what the network infers: detecting adversarial examples based on semantic contradiction. In *The Network and Distributed System Security Symposium (NDSS)*, 2022.
- [88] Zhiyuan Yu, Yuanhaur Chang, Ning Zhang, and Chaowei Xiao. SMACK: Semantically meaningful adversarial audio attack. In *32nd USENIX Security Symposium (USENIX Security 23)*, pages 3799–3816, 2023.
- [89] Jiawei Zhang, Zhongzhu Chen, Huan Zhang, Chaowei Xiao, and Bo Li. DiffSmooth: Certifiably robust learning via diffusion models and local smoothing. In *32nd USENIX Security Symposium (USENIX Security 23)*, pages 4787–4804, 2023.
- [90] Shibo Zhang, Yushi Cheng, Wenjun Zhu, Xiaoyu Ji, and Wenyuan Xu. CAPatch: Physical adversarial patch against image captioning systems. In *USENIX Security Symposium*, pages 679–696, 2023.
- [91] Shigeng Zhang, Shuxin Chen, Chengyao Hua, Zhetao Li, Yanchun Li, Xuan Liu, Kai Chen, Zhankai Li, and Weiping Wang. Lsd: Adversarial examples detection based on label sequences discrepancy. *IEEE Transactions on Information Forensics and Security*, 2023.
- [92] Xinyang Zhang, Ningfei Wang, Hua Shen, Shouling Ji, Xiapu Luo, and Ting Wang. Interpretable deep learning under fire. In *Usenix Security Symposium*, 2020.
- [93] Dawei Zhou, Yukun Chen, Nannan Wang, Decheng Liu, Xinbo Gao, and Tongliang Liu. Eliminating adversarial noise via information discard and robust representation restoration. In *International Conference on Machine Learning*, pages 42517–42530. PMLR, 2023.
- [94] Boyu Zhu, Changyu Dong, Yuan Zhang, Yunlong Mao, and Sheng Zhong. Towards universal detection of adversarial examples via pseudorandom classifiers. *IEEE Transactions on Information Forensics and Security*, 2023.
- [95] Hong Zhu, Shengzhi Zhang, and Kai Chen. AI-guardian: Defeating adversarial attacks using backdoors. In *2023 IEEE Symposium on Security and Privacy (SP)*, pages 701–718. IEEE Computer Society, 2023.

APPENDIX A ADVERSARIAL EXAMPLE ATTACK

- **Image Modality.** The 7 AE attacks evaluated in section 4 are briefly introduced, which include 6 white-box attacks and 1 black-box attack. Specifically, the white-box adversarial examples include Fast Gradient Sign Method (FGSM) [26], Projected Gradient Descent (PGD) [49], Basic Iterative Method (BIM) [37], Carlini and Wagner Attack (CW) [13], DeepFool [54], Jacobian Saliency Map Attack (JSMA) [57]. The black-box adversarial example attack is Boundary attack [11].

FGSM computes delicate perturbations to be added to the input example by leveraging the gradients of a target model to maximize loss, causing misclassification without compromising the original example semantic notably. The perturbation is injected within only one-step. BIM also known as iterative FGSM, is an iterative variant of the FGSM, which operates by applying FGSM iteratively to generate adversarial examples. PGD works similarly to BIM, extending FGSM by employing multiple iterations or steps of gradient descent while projecting the perturbation onto an ϵ -ball (a range or boundary) around the original example to ensure the perturbation remains close to the original example and within a bounded region. CW is an optimization-based adversarial attack method that formulates the AE generation as an optimization problem, aiming to find perturbations that minimize the distortion while ensuring misclassification, often considered one of the most effective and versatile AE attacks. DeepFool is an iterative adversarial attack method that computes minimal perturbations by iteratively linearizing the target model’s decision boundary to find the shortest distance from an input image to misclassify it, making it highly effective in generating imperceptible adversarial perturbations. JSMA leverages the Jacobian matrix of a neural network to identify and craft adversarial perturbations by exploiting the sensitivity of the model’s decision boundaries to small changes in input features, aiming to deceive the model into misclassification while considering the input’s saliency information. Boundary Attack as a black-box attack starts from a randomly chosen point near the decision boundary of a victim model and iteratively moves towards the target classification boundary by performing small perturbations.

- **Text Modality.** To evaluate TRAIT performance on textual modality in subsection 5.2, we consider four mainstream textual AE attacks: Projected Word-Wise Substitution (PWWS) [61], TextBugger [40], HotFlip [21], UAT [77]. PWWS, HotFlip, and UAT are white-box attacks and TextBugger is a black-box attack.

PWWS [61] aims to generate perturbations in text by substituting words with their semantically similar counterparts while ensuring these changes are imperceptible to human readers. Unlike PWWS, TextBugger [40] also makes word substitution and employs various transformations, including synonym substitution, addition, and modification, to craft adversarial examples, thereby showcasing a broader range of attack strategies in the textual modality. HotFlip [21] is an adversarial attack method for text classification that operates in a white-box setting, focusing on substituting individual words in the input text to alter the

classification decision of a model. It utilizes gradient information to find the most influential words to flip, aiming to generate minimal perturbations that cause misclassification. In contrast to PWWS and TextBugger, HotFlip primarily focuses on flipping words rather than employing a broader range of transformations, emphasizing a more targeted approach to crafting adversarial examples in the textual modality based on word-level perturbations and gradients. Compared to PWWS, TextBugger, and HotFlip, the strength of UAT (Universal Adversarial Triggers) [77] lies in its ability to create universal perturbations that have consistent adversarial effects across different inputs and models.

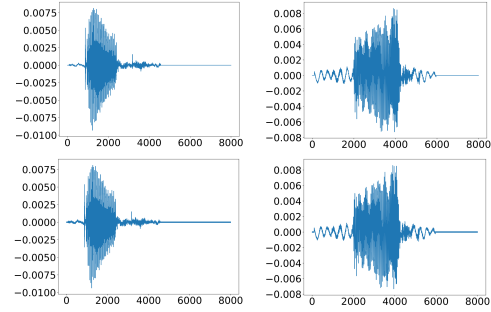


Figure 14: (Top) Benign audio waveform and (Bottom) its (Below) corresponding adversarial audio waveform. AE method of (Left) FGSM, and (Right) PGD.

Table 6: TRAIT detection performance when synthetic loss computed using every two constructive IMs (CI-FAR10+VGG16).

AE Attack Method	Preset FRR(%)	AE Acc(%)	
		Conse.	Prev.
FGSM ($\epsilon = 8/255$)	1	98.57	99.01
	3	98.72	99.33
	5	98.95	99.41
PGD ($\epsilon = 8/255$)	1	98.15	98.79
	3	98.48	99.11
	5	98.54	99.24
CW	1	99.37	99.64
	3	99.45	99.81
	5	99.52	99.86

APPENDIX B AE COUNTERMEASURE

To counter notorious AE attacks, three main approaches can be leveraged, which are: modifying the model and changing the training process; input transformation to eliminate the attack effect; and AE detection.

Model/Training Modification. Adversarial training [50], [60], [65] dominates this categorization, where AEs are included in the training data to learn features against them—regularization that changes the default training process is often applied. This approach is bound together with the target DL model. Hence, re-training is required if the classifier changes and the cost of adversarial training increases for a more complicated DL model. Some works require modifying the model architecture, e.g., accommodate to add an outlier class [28] and then retraining the underlying model—the retraining needs knowledge of *seen adversarial examples*.

Besides retraining, the generation of AEs in the training exacerbates computational costs. In addition, observation of crafted AEs is a prerequisite for adversarial training, which is thus susceptible to unseen AE attacks. Moreover, model architecture modification or training regularization could often hurt the model performance (e.g., degrading accuracy) on benign examples [28], [60].

Input Transformation. The manipulation of input can be achieved using diverse methods such as JPEG compression [20], [44], bit reduction [29], [86], pixel deflection [59], or employing random transformations [82]. Beyond defenses operating within pixel space, malevolent images can also be reconstructed to better adhere to natural image statistics through the use of e.g., generative models [64], [93]. However, these transformations unavoidably impact benign examples, leading to a compromise between the accuracy of benign examples and the efficacy of mitigating adversarial effects. It’s crucial to note that these transformations are primarily tailored for specific imaging modalities, potentially making them unsuitable or challenging to implement in other modalities. Furthermore, these methods cannot detect the AE attack, identify the attack source and the attacker, and provide no deterrence to attackers.

Adversarial Detection. The exploration of input example’s neighborhood information, such as local intrinsic dimensionality [47], has served as a fundamental basis in numerous studies aiming to detect AEs [17], [23], [33], [39], [56], [73]. However, the training of the detector (referred to as the meta-classifier) in these detection studies [2], [23], [47], [56], [73] necessitates the observation of AEs, rendering them highly vulnerable to unseen AE attacks. Additionally, this approach can lead to significant computational overhead due to the requirement of substantial neighborhood information [2].

LSD [91] and NIC [46] assess the inconsistency of a DL model’s intermediate layers predicted labels to detect AEs. These defenses add internal classifiers to intermediate layers of the model e.g., CNN model, to obtain predictions from internal classifiers. ContraNet [87] utilizes a class-conditional GAN to reconstruct an incoming image based on its predicted label, leveraging semantic similarity between the reconstructed and original images to identify AEs that demonstrate lower similarity. Similar to prior work such as [86], it incurs a sacrifice in accuracy for benign images to some extent. Meanwhile, uGuard [10] concentrates on detecting unsafe images, such as those containing explicit content, within social networks. Upon detection of such images, it employs interpretability to obfuscate the harmful content. It’s important to note that while [30] advocates for interpretability as an AE countermeasure, it remains potentially vulnerable to AE attack variant [92].

Input preprocessing can be used to detect AEs. Feature Squeezing [86] constructs an AE detector by checking the inconsistency of inference results when the input has undergone differing squeezing operations. ADDITION [79] introduces random noise into the input image and subsequently reconstructs it for denoising purposes. The denoised image is then compared with the original input image; if a prediction inconsistency beyond a certain threshold is detected, the input is deemed adversarial. However, this method proves ineffective when the adversarial perturbation is not

exceedingly small while still remaining imperceptible.

Certiably AE detection methods [68], [80], [81] stand out due to their capability of providing provable detection under assumed bounds, such as perturbation magnitude, in contrast to other approaches. However, this method often incurs heavy computational requirements and can be easily compromised, as attackers are not obliged to adhere to the underlying assumptions, such as constrained small perturbations or specific norms like ℓ_∞ .